PARAMETRIC INTERPOLATION TO SCATTERED DATA

AZIZAN BIN SAABAN

UNIVERSITI SAINS MALAYSIA

2008

PARAMETRIC INTERPOLATION TO SCATTERED DATA

by

AZIZAN BIN SAABAN

Thesis submitted in fulfilment of the requirements for the degree of Doctor of Philosophy

May 2008

ACKNOWLEDGEMENTS

I would like to express my sincere thanks to my supervisors Associate Professor Dr. Ahmad Abd. Majid and Associate Professor Dr. Abd. Rahni Mt. Piah of Universiti Sains Malaysia, and my field supervisor Associate Professor Dr. Lawrence Hooi Tuang Chang of Universiti Malaysia Perlis for their guidance, suggestions, invaluable advice and patience throughout my Ph.D work and in completing this thesis.

My sincere appreciation to Universiti Sains Malaysia especially the Dean of the School of Mathematical Sciences and the Dean of Institute of Graduate Studies for allowing me to pursue my higher degree here.

I also gratefully acknowledge to the Ministry of Higher Education of Malaysia and the Universiti Utara Malaysia for providing me the financial assistance during my study.

I would also extend my gratitude to the Hydro Geomorphology Research Group of Humanities Section in School of Humanities, Universiti Sains Malaysia, the Malaysian Geosciences Department and the Malaysian Meteorology Department for providing the actual data used in this thesis.

Most of all, I would also thank to my wife Rosmawati Che Din, my daughters Farah Lina, Fatin Aina, Farhanah, Fasya Fasihah and Fatimah Najah, and my son Muhammad Nur Iman for their love and moral support.

TABLE OF CONTENTS

		Page
ACKNOWLEDGEMENTS		ii
TABLE OF CONTENTS		iii
LIST OF TABLES		vi
LIST OF FIGURES		vii
ABSTRAK		xii
ABSTRACT		xiv
CHAPTER 1 - INTRODUCTION		1
1.1	Interpolation to General Scattered Data	1
1.2	Interpolation to Positive Scattered Data	8
1.3	Thesis Outline	12
CHAPTER 2 – BACKGROUND		14
2.1	Introduction	14
2.2	Triangulation of Data Points	14
2.3	Gradient Estimation Methods	16
	2.3.1 Convex Combination Method	17
	2.3.2 Method Based on Least Square Minimization	20
2.4	Representation with Bézier Triangular Patches	22
	2.4.1 Barycentric Coordinates	22
	2.4.2 Bézier Triangular Patches	23
	2.4.3 Derivatives of Bézier Triangular Patches	24
2.5	Smoothness Conditions	24
	2.5.1 Parametric Continuity	25
	2.5.2 Geometric Continuity	26

CHAPTER 3 - SURFACE INTERPOLATION ON A TRIANGLE USING CONVEX COMBINATION METHOD 28

3.1 Introduction 28

3.2 Convex Combination Method 28

3.3 C^1 Cubic Triangular Interpolant 30

3.3.1 Calculation of Edge Ordinates 32

3.3.2 Calculation of Inner Ordinates b_{111}^i, $i = 1,2,3$ using Linear Cross Boundary Derivatives Method 33

3.3.3 Calculation of Inner Ordinates b_{111}^i, $i = 1,2,3$ using Cubic Precision Method 34

3.3.4 Interpolating Surface 36

3.4 C^2 Quintic Triangular Interpolant 37

3.4.1 Calculation of b_{410}, b_{401}, b_{320}, b_{302}, b_{311}, b_{140}, b_{041}, b_{230}, b_{032}, b_{131}, b_{104}, b_{014}, b_{203}, b_{032} and b_{113} Ordinates 39

3.4.2 Calculation of Inner Ordinates b_{122}^i, b_{212}^i, b_{221}^i, $i = 1,2,3$ 41

3.4.3 Interpolating Surface 44

CHAPTER 4 - SURFACE INTERPOLATION ON A TRIANGLE WITH MINIMIZED PRINCIPAL CURVATURE NORM 45

4.1 Introduction 45

4.2 C^1 (or G^1) Quartic Triangular Interpolant 46

4.2.1 C^1 Conditions Between Adjacent Quartic Patches 47

4.2.2 G^1 Conditions Between Adjacent Quartic Patches 49

4.3 Surface with Minimized Principal Curvarture Norm 50

4.4 Graphical Examples 60

4.5 Error Analysis 68

CHAPTER 5 - POSITIVITY PRESERVING INTERPOLATION 75

5.1 Introduction 75

5.2 Sufficient Positivity Conditions on Degree-*n* Bezier Triangular Patch 76

5.3 Sufficient Positivity Conditions on Quintic Bezier Triangular Patch and Its Construction 84

5.3.1 Positivity Conditions 84

5.3.2 Construction of C^2 Positivity-preserving Interpolating Surface 85

5.4 An improved Positivity conditions on Cubic Bézier Triangular Patch and Its Construction 94

5.4.1 Sufficient Positivity-preserving Conditions on Boundary Curves of Degree-*n* Bézier Triangular Patch 94

5.4.2 Sufficient Positivity-preserving Conditions on Cubic Bézier Triangular Patch 99

5.4.3 Construction of Positivity Preserving Interpolating Surface using Convex Combination of Cubic Bézier Triangular Patches 106

5.5 Graphical Examples 111

5.5.1 Examples using Test Functions 111

5.5.2 Application on Real Data 123

5.5.2.1 Visualization of Peninsular Malaysia Rainfall Pattern 123

5.5.2.2 Visualization of Kelantan Geochemical Distribution Pattern 131

CHAPTER 6 - CONSTRAINED INTERPOLATION 138

6.1 Introduction 138

6.2 Construction of C^2 Constrained Interpolating Sufaces using Quintic Bézier Triangles 138

6.3 Data points above or under Constraint Surface 143

6.4 Data Points between Two Constraint Surfaces 152

CHAPTER 7 - CONCLUSIONS AND FUTURE RESEARCH 158

REFERENCES 161

APPENDICES

APPENDIX A Test functions and data set used in Sections 3.3.4, 3.4.3 and 4.4

APPENDIX B Test functions and data set used in Section 5.5.1

APPENDIX C Actual data points used in Section 5.5.2

APPENDIX D Data set used in Sections 6.3 and 6.4

PUBLICATIONS LIST

LIST OF TABLES

		Page
Table 4.1	Error norms on node set 1	71
Table 4.2	Error norms on node set 2	71
Table 4.3	Error norms on node set 3	72
Table 4.4	Error norms on node set 4	72
Table 4.5	Error norms on node set 5	72
Table 5.1	Maximum and mean errors (test function F_1)	113
Table 5.2	Maximum and mean errors (test function F_2)	117
Table 5.3	Maximum and mean errors (test function F_3)	118
Table 5.4	Maximum and mean errors (test function F_4)	122
Table 5.5	Minimum value of the test functions for non-positivity and positivity preserved methods	122
Table 5.6	Minimum value of average rainfall for non-positivity and positivity-preserved methods	125
Table 5.7	Minimum value of Co and Cu concentrations for non-positivity and positivity preserved methods	133

LIST OF FIGURES

		Page
Figure 2.1	(a) Voronoi diagram (b) Delaunay triangulation with its Voronoi diagram (c) Delaunay triangulation (d) Concept of Delaunay triangulation	16
Figure 2.2	Triangles in a triangulation ($k = 5$)	17
Figure 2.3	Vector plane of linear interpolant to the data at vertices of T_i	18
Figure 2.4	Node V on the boundary of the domain	19
Figure 2.5	k vertices surrounding vertex P	20
Figure 2.6	Barycentric coordinates	23
Figure 2.7	Two triangles with a common boundary	25
Figure 2.8	A configuration of two parallel rows of adjacent quartic patches	27
Figure 3.1	Nielson's side-vertex interpolant	29
Figure 3.2	Cubic Bézier triangular patch	30
Figure 3.3	Vertices and edges of a triangle element	31
Figure 3.4	Inward normal direction to the edges of triangle	33
Figure 3.5	Two adjacent cubic triangular patches	34
Figure 3.6	C^1 Surface interpolation (data points from function F_1) (a) Goodman and Said's approach (b) Foley and Optiz's approach	37
Figure 3.7	C^1 Surface interpolation (data points from function F_2) (a) Goodman and Said's approach (b) Foley and Optiz's approach	37
Figure 3.8	Quintic Bézier triangular patch	38
Figure 3.9	Adjacent quintic triangular patches	43
Figure 3.10	C^2 surface interpolation (a) data points from function F_1 (b) data points from function F_2	44
Figure 4.1	Bezier ordinates of a quartic triangular patch	46

Figure 4.2	Control points of adjacent quartic triangular patches	48
Figure 4.3	Parametric tranformation	53
Figure 4.4	C^1 quartic surface interpolation from function F_1 (a) 36 data points (b) 65 data points (c) 100 data points	61
Figure 4.5	Contour plot of an actual F_1 surface	62
Figure 4.6	Contour plot of F_1 surface (36 data points) (a) our method (b) *GH*-C^1 method (c) *FO*-C^1 method (d) *CH*-C^2 method	62
Figure 4.7	Contour plot of F_1 surface (65 data points) (a) our method (b) *GH*-C^1 method (c) *FO*-C^1 method (d) *CH*-C^2 method	63
Figure 4.8	C^1 quartic surface interpolation from function F_2 (a) 36 data points (b) 65 data points (c) 100 data points	64
Figure 4.9	Contour plot of an actual F_2 surface	65
Figure 4.10	Contour plot of F_2 surface (36 data points) (a) our method (b) *GH*-C^1 method (c) *FO*-C^1 method (d) *CH*-C^2 method	65
Figure 4.11	Contour plot of F_2 surface (65 data points) (a) our method (b) *GH*-C^1 method (c) *FO*-C^1 method (d) *CH*-C^2 method	66
Figure 4.12	Digital elevation data of Kalumpang Agricultural Station (a) triangulation domain (b) linear interpolant (c) interpolating surface	67
Figure 4.13	Test functions	69
Figure 4.14	Triangulation domain of node sets on square grid [0,1]x[0,1]	70
Figure 4.15	Average coefficient of determination value, r^2 for node sets 1-5	73
Figure 4.16	Average coefficient of determination value r^2 for node sets 1,4,5	73
Figure 4.17	Average coefficient of determination value, r^2 for node sets 2, 3	73
Figure 5.1	Function $G(s)$, $s \geq 0$ for degree-n Bézier triangular patch	80
Figure 5.2	Function $G(s)$, $s \geq 0$ for cubic Bézier triangular patch	82
Figure 5.3	Function $G(s)$ with $s \geq 0$ for quintic Bézier triangular patch	85
Figure 5.4	Triangles in triangulation with the common vertex O	86
Figure 5.5	Function $G(s)$ with $s \geq 0$ for degree-n Bézier polynomial curve	97
Figure 5.6	Lower bound of Bezier ordinates for cubic triangular patch	100
Figure 5.7	The unique solution of $f(t)= 0$ in $(0, b_0 + b_3)$	102

Figure 5.8	Triangulation domain (a) 36 node points (b) 63 node points (c) 26 node points (d) 100 node points	111
Figure 5.9	C^2 quintic interpolating surface (data set 1) (a) without positivity-preserved (b) with positivity-preserved from Corrollary 5.1	113
Figure 5.10	C^1 cubic surface (data set 1) (a) without positivity-preserved (b) with positivity-preserved from Proposition 5.4	114
Figure 5.11	C^2 quintic surface (data set 2) (a) without positivity-preserved (b) with positivity-preserved from Corrollary 5.1	115
Figure 5.12	C^1 cubic surface (data set 2) (a) without positivity-preserved (b) with positivity-preserved from Proposition 5.4	116
Figure 5.13	C^2 quintic surface (data set 3) (a) without positivity-preserved (b) with positivity-preserved from Corrollary 5.1	118
Figure 5.14	C^1 cubic surface (data set 3) (a) without positivity-preserved (b) with positivity-preserved from Proposition 5.4	119
Figure 5.15	C^2 quintic surface (data set 3) (a) without positivity preserved (b) with positivity-preserved from Corrollary 5.1	120
Figure 5.16	C^1 cubic surface (data set 3) (a) without positivity preserved (b) with positivity preserved from Proposition 5.4	121
Figure 5.17	Triangulation domain of rainfall measurement stations in Peninsular Malaysia	124
Figure 5.18	Linear interpolant for the average rainfall of Peninsular Malaysia (March 2007)	124
Figure 5.19	Linear interpolant for the average rainfall of Peninsular Malaysia (May 2007)	125
Figure 5.20	C^2 Interpolating surfaces for the average rainfall of Peninsular Malaysia (March 2007) (a) without positivity-preserved (b) with positivity-preserved	127
Figure 5.21	C^1 Interpolating surfaces for the average rainfall of Peninsular Malaysia (March 2007) (a) without positivity-preserved (b) with positivity-preserved	128
Figure 5.22	C^2 Interpolating surfaces for the average rainfall of Peninsular Malaysia (May 2007) (a) without positivity-preserved (b) with positivity-preserved	129
Figure 5.23	C^1 Interpolating surfaces for the average rainfall of Peninsular Malaysia (May 2007) (a) without positivity-preserved (b) with positivity-preserved	130
Figure 5.24	149 sampling locations	131

Figure 5.25	Triangulation domain of 149 sampling locations	132
Figure 5.26	Linear interpolant of Co concentration	132
Figure 5.27	Linear interpolant of Cu concentration	132
Figure 5.28	C^2 quintic interpolating surfaces of Co concentration (a) without positivity-preserved (bottom view) (b) with positivity-preserved (top view)	134
Figure 5.29	C^1 quintic interpolating surfaces of Co concentration (a) without positivity-preserved (bottom view) (b) with positivity-preserved (top view)	135
Figure 5.30	C^2 quintic interpolating surfaces of Cu concentration (a) without positivity-preserved (bottom view) (b) with positivity-preserved (top view)	136
Figure 5.31	C^1 quintic interpolating surfaces of Cu concentration (a) without positivity-preserved (bottom view) (b) with positivity-preserved (top view)	137
Figure 6.1	Data points above constraint surface	142
Figure 6.2	Data points below constraint surface	142
Figure 6.3	Data points between two constraint surfaces	143
Figure 6.4	Positivity interpolating surface (Figure 5.9) together with the upper constraint z =1	146
Figure 6.5	Constrained interpolating surface together with upper constraint z =1	146
Figure 6.6	True surface of $g(x, y)$	147
Figure 6.7	The unconstrained interpolating surface together with lower bound linear surface	148
Figure 6.8	The constrained interpolating surface together with lower bound linear surface	148
Figure 6.9	The unconstrained interpolating surface together with lower bound quadratic surface	149
Figure 6.10	The constrained interpolating surface together with lower bound quadratic surface	149
Figure 6.11	The unconstrained interpolating surface together with lower bound quintic surface	150
Figure 6.12	The constrained interpolating surface together with lower bound quintic surface	150

Figure 6.13	The unconstrained interpolating surface together with upper bound cubic surface	151
Figure 6.14	The constrained interpolating surface together with upper bound cubic surface	151
Figure 6.15	The unconstrained interpolating surface together with upper bound quartic surface	152
Figure 6.16	The constrained interpolating surface together with upper bound quartic surface	152
Figure 6.17	The unconstrained interpolating surface together with upper bound quartic surface and lower bound quadratic surface	156
Figure 6.18	The constrained interpolating surface together with upper bound quartic surface and lower bound quadratic surface	156
Figure 6.19	The unconstrained interpolating surface together with upper bound cubic surface and lower bound quintic surface	157
Figure 6.20	The constrained interpolating surface together with upper bound cubic surface and lower bound quintic surface	157

INTERPOLASI BERPARAMETER KE ATAS DATA TERSEBAR

ABSTRAK

Dua skema interpolasi berparameter yang mengandungi interpolasi global untuk data tersebar am dan interpolasi pengekalan-kepositifan setempat data tersebar positif dibincangkan. Skema-skema ini telah dibina menggunakan tampalan-tampalan segi tiga Bézier cebis demi cebis.

Skema pertama membincangkan pembinaan kaedah interpolasi global berasaskan ukuran kesaksamaan norma kelengkungan utama yang akan mnjana satu permukaan bernorma kelengkungan utama minimum. Permukaan ini terdiri daripada segi tiga Bézier kuartik cebis demi cebis yang memenuhi kekangan-kekangan interpolasi sempadan tampalan dan juga memberikan kebebasan kepada sebahagian daripada titik-titik kawalan untuk digunakan sebagai pembagusan permukaan.

Fungsi objektif ditakrifkan sebagai fungsian bentuk kuadratik dan nilai ekstremum bagi fungsian ini terhadap syarat-syarat keselanjaran C^1 merentasi sisi-sisi sepunya dan pada bucu-bucu segi tiga akan diperoleh. Kaedah pengoptimum dengan pendaraban Lagrange digunakan bagi mendapatkan titik-titik Bézier anu untuk keseluruhan jaringan segi tiga dan permukaan-permukaan interpolasi optimum dapat dibina.

Skema kedua membincangkan interpolasi pengekalan-kepositifan setempat untuk data tersebar positif menggunakan tampalan-tampalan segi tiga Bézier cebis demi cebis dengan mengenakan batas bawah ordinat-ordinat Bézier. Skema pengekalan-kepositifan teritlak untuk segi tiga Bézier darjah-n diterbitkan dan interpolasi pengekalan-kepositifan C^2 kuintik menggunakan kaedah gabungan cembung yang memerlukan input sehingga terbitan-terbitan separa peringkat kedua pada titik-titik data telah dibina. Batas bawah bagi ordinat-ordinat Bézier pada setiap

segi tiga diumpukkan nilai yang sama. Pendekatan ini telah diperluas kepada masalah interpolasi berkekangan yang meliputi permukaan-permukaan kekangan sehingga polinomial berdarjah lima.

Kami juga mencadangkan interpolasi pengekalan-kepositifan C^1 kubik baru dengan memberikan lebih kelenturan ke atas batas bawah ordinat-ordinat Bézier, yang mana ordinat-ordinat sisi untuk tampalan segi tiga diubahsuai secara bebas manakala ordinat dalam bersandar kepada ordinat-ordinat sisi. Pendekatan baru ini menghasilkan masalah pengoptimum dengan kekangan.

Contoh-contoh grafik menggunakan fungsi-fungsi ujian terkenal dan data sebenar telah dipersembahkan.

PARAMETRIC INTERPOLATION TO SCATTERED DATA

ABSTRACT

Two schemes of parametric interpolation consisting of a global scheme to interpolate general scattered data and a local positivity-preserving scheme to interpolate positive scattered data are described. These schemes are constructed using piecewise triangular Bézier patches.

The first scheme deals with the construction of a global interpolating method based on fairness measure of principal curvature norm that will generate a final surface with minimized principal curvature norm. The final surface comprises of piecewise quartic Bézier triangles which satisfy the patch boundary interpolation constraints as well as allow certain freedom to some of their control points used in surface fairing.

An objective function is defined using a quadratic functional form and the extremum of this functional with respect to the C^1 continuity conditions along the shared edges and vertices of triangle is obtained. A Lagrange multiplier optimization method is used to obtain the unknown Bézier points for the entire triangular mesh and subsequently optimizes the interpolating surface which is then generated.

The second scheme describes a local positivity-preserving interpolation to positive scattered data using piecewise Bézier triangular patches by imposing a lower bound on the Bézier ordinates. The generalised positivity-preserving scheme for triangular Bézier patch of n degree is derived and a C^2 quintic positivity-preserving interpolation using a convex combination method with inputs up to the second order partial derivatives at data points is constructed. The lower bound of all Bézier ordinates in a corresponding triangle (except for the vertices) are assigned the same

value. This approach is then extended to the constrained interpolation problem by allowing polynomials of up to degree five as constraint surfaces.

We also suggest a new C^1 cubic positivity-preserving interpolation by imposing more flexibility on the lower bound of Bézier ordinates, where the edge ordinates of a triangular patch are adjusted independently while the inner ordinate depends on these edge ordinates. This new approach leads to a constrained optimization problem.

Examples are illustrated graphically using well-known test functions and actual data.

CHAPTER 1
INTRODUCTION

Scattered data interpolation refers to the problem of fitting smooth surfaces through a non-uniform distribution of data points. In practise, this subject is very important in various sciences and engineering where data are often measured or generated at sparse and irregular positions. The goal of interpolation is to construct underlying functions which may be evaluated at certain set of positions. There are various principal sources of scattered data, for examples measured value of physical quantities such as in geology, meteorology, oceanography, cartography and mining; experimental results in sciences and engineering; computational values in various applications of computer graphics and vision with functional data; medical imaging and others. Numerous interpolation methods with many variants have been devised to solve the problem of scattered data interpolation in two or more independent variables. They have been addressed in many papers and book chapters (see [91], [5], [29], [30], [24], [32], [28], [63]) that are dispersed in various scientific disciplines. It should be noted that the concepts involved in scattered data interpolation are largely inspired from the fundamental concepts in the interpolation of regularly spaced data.

1.1 Interpolation to General Scattered Data

The different approaches to the interpolant schemes of scattered data can be classified into global methods, in which each interpolated value is influenced by all the data, and local methods, in which the interpolated value is only influenced by the values at nearby points from the scattered point set. Global methods are practically limited to small data sets due to the computational efforts they require; moreover, an addition or deletion of a data point, or a correction in any of the coordinates of a data

point, will modify the interpolated values throughout the entire domain of definition. Local methods, on the other hand, are capable of treating much larger data sets, and they are less sensitive to data modifications, but they may become quite complex, too, if a smooth result is required.

One of the earliest interpolating schemes was based on inverse distance weighting of data developed by Shepard [93] which is known as Shepard's method. Shepard defined a C^0 interpolant as a weighted average of the data with weights being inversely proportional to distance. This method suffers from several defect including cusp, corners and flat spots at data points as well as undue influence of points which are far away. In addition, it is a global scheme requiring all the weights to be recomputed if any data point is added, removed or modified. To address these deficiencies, Franke and Nielson [29], introduced a C^1 interpolant scheme by modifying this quadratic Shepard's method, which is also known as Modified Shepard's Method. This variation modifies the weighting function by only considering the points lying in a disc with radius and centered at the point of evaluation. The modification improves the earlier Shepard's method in addressing the preservation of the shape near the data points and in making it to be local to a neighbourhood point.

Another popular approach is to define the interpolant as a linear combination of radially symmetric basis functions each centered at a data point. The radial interpolant is translation and rotation invariant. The unknown coefficients for the basis functions are determined by solving a linear system of equations where the coefficient matrix is always full, but may become poorly conditioned and require preconditioning for a large data set (see [19], [20]). The popular choice for the basis functions is due to its very well performed in practical application including

Gaussian and multiquadratics ([45]), shifted log ([32], [47]) and thin plate splines ([31], [64]). The previous two methods mentioned do not involve any prior meshing that is rectangulation or triangulation step and can be thought of as meshless.

Another way to construct an interpolant to general scattered data is to triangulate the domain data points in the plane and construct piecewise parametric or geometric continous interpolant on each triangle. This method is referred to as triangulation-based method and is one of the main objectives of this thesis. Piecewise or rational interpolants of low degree using triangular Bézier patches representation are very popular and successful for arbitrary scattered data. Bézier triangles are extensively used in the area of Computer Aided Geometric Design with an excellent description of Bézier curves and surfaces given in Farin [24]. Each triangular patch bounded by three curves is filled in by one or more polynomial or rational surface patches in such a way that the overall surface is of parametric or geometric continuous. The main challenge to implement this scheme is to construct a smooth interpolant of low degree with as few pieces as possible. There are several major approaches to fill these triangular patches.

The first approach is a polynomial interpolating method given by Farin [24]. Farin constructed a piecewise polynomial interpolant over a triangulation that generates C^r surfaces. Each interpolant is local and determined by the linear or non-linear functionals that are defined over one triangle only. Generally, a local interpolant is a polynomial of degree that depend on r which interpolates to all its derivatives of up to order r of some primitive function f at the vertices of a triangulation. Based on a well-known finite element method called condensation of parameters, Whelan [99] presented a C^2 piecewise nonic interpolants of condensed and uncondensed schemes using Berstein-Bézier method. The constructed interpolant

requires only vertex data and its derivatives which have seventh degree polynomial precision for condensed scheme and ninth degree polynomial for the uncondensed scheme. Whelan's interpolation scheme is more useful in the area of finite element analysis as compared to in the other areas.

Another approach was based on the discrete-triangular method ([3], [62]). Alfeld and Barnhill [3] proposed a transfinite C^2 interpolation scheme through the discretization of the transfinite scheme by deriving two different finite dimensional C^2 interpolants which is rather complicated. This approach was further studied by Liu and Zhu [62] who also described a characterization of certain C^2 discrete triangular interpolants. They created two different C^2 discrete triangular interpolants i.e. with quintic precision and with cubic precision respectively, which are much more concise in their forms as compared to those by Alfeld and Barnhill, and hence more convenient for practical use. Moreover, these interpolants are of explicit forms, therefore need not have to solve a linear system and are easy to calculate and analyze.

The next popular method of filling the triangular patches is a split-triangle method known as Clough-Tocher interpolant which has been widely discussed in Farin ([23], [24]) and Alfeld [2]. Each macro-triangle is split into three triangles by inserting a point in the interior of the triangle and then connect it to the three vertices of original triangle. This splitting technique therefore fits three patches for each triangle. Splitting allows the data along each boundary to be matched independently of the data on the other two boundaries. This method uses bivariate cubic polynomials within each triangle. Hence, the key idea behind the Clough–Tocher's method is to split each cubic polynomial patch into three cubic polynomial subpatches in order to satisfy the C^1 continuity constraints with neighbours.

Specifically, a cubic Bézier patch is defined over each mini-triangle. This technique has been used to construct three polynomials of degree four per triangle hole with G^1 continuity ([95], [51]) and with C^1 continuity ([76]).

Another method of split-triangle is known as Powell-Sabin split ([80]). The method produces C^1 piecewise quadratic interpolants to C^1 data at vertices of a triangulated data. Each triangle patch is splitted into six or twelve mini-triangles determined by triangle geometry. For the case of a six-triangle split, the macro triangle is split by joining the centre of the circumscribed circle to edge midpoints. Otherwise in twelve-triangle split, the macro-triangle is split by joining its centroid to the edge midpoints and by joining the edge midpoints to one another. Then, piecewise quadratic patch is built on each mini-triangle in order to satisfy C^1 continuity constraints with its neighbours.

Recently, Hahmann and Bonneau [43] introduced a new interpolation method that avoids undulations, even when interpolating irregular triangulations. This method allows free choice of all first derivatives at each input vertex, along each input edge. Each input triangle is regularly subdivided into four sub-triangles and a degree 5 Bézier patch is associated to each of the sub-triangles. These four Bézier patches are referred to as a macro-patch. Inside a macro-patch, the four Bézier patches are connected with C^1 continuity while the macro-patches are themselves connected with G^1 continuity.

An alternative method to fill the triangular patch without splitting the triangle is by a convex-combination method which will be used throughout this thesis. This interpolation scheme creates one single patch per hole. First, three patches are constructed, each of which interpolates part of the boundary data. Then a convex combination of the three patches is formed in such a way that the resulting patch

interpolates all the data. The convex combination method typically utilizes rational weight functions ([69], [46], [61]) and therefore produces rational interpolants. Gregory [37] was the first to introduce the convex combination method in Computer Aided Geometric Design and later on was further developed in Gregory [38] ,and Charrot and Gregory [16]. These methods are based upon the combination of interpolation operators consisting of univariate interpolation along the lines parallel to the sides of a triangle.

Besides the above-mentioned works, Nielson [69] presented a side-vertex method for constructing a curved triangular patch using combination of three interpolating operators, each satisfying the given interpolation conditions at a vertex and its opposite sides. Hagen [40] developed a method of constructing geometric surface patches based on Nielson's approach and the results have been generalized to triangular surface patches with first and second order geometric continuity in Hagen and Pottmann [41], and Nielson [72].

Moreover, in the scattered data interpolation area, Foley and Optiz [27], and Goodman and Said [35] independently developed a C^1 cubic triangular convex combination scheme. Chang and Said [15] further extended this approach to C^2 quintic triangular surface scheme that requires up to the second-order partial derivative values. Most recently, Zhang and Cheng [101] described a new method for constructing C^1 triangular patches that interpolates a given boundary curve and cross-boundary slopes by blending three side-vertices of Nileson's interpolation operator [69] with a new interior operation operator based on three quartic curves. Thus, this approach presents a method to construct a curved triangular patch by combining four interpolating operators and the constructed triangular patch which reproduced polynomial surfaces of degree four.

One of the major findings to fill a triangular hole using a local interpolant method is that most of these schemes suffer from similar shape defects caused mainly by the construction of boundary curves. Shape defects in boundary curves such as flatness seems to be propagated inward resulting in the flat spots of the surfaces ([63]). One way to overcome this problem is to use several global optimality fairness criteria based on variational principle method which have been introduced. It allows the design of very smooth surfaces satisfying a number of interpolation constraints. The important point of the method is to choose a suitable objective function, whose value is determined by the variables that also determine the surface shape (e.g., the control points of a Bézier surface). An objective function must attains a minimum value when the shape variables assume values that correspond. The fairness criteria of surfaces such as principal curvature, Gaussian curvature, mean curvature, absolute curvature or principal curvature norm ([100]) were used as the objective functions to be minimized. These criteria can be described in terms of the distribution of its second and higher order derivatives, preferably expressed as geometrically invariant surface properties. There is a large number of curve and surface fairing techniques that uses some degree of optimization.

In the case of scattered data interpolation, Nielson [70] introduced the minimum-norm network (MNN) using a linear energy term to produce a C^1 cubic network and resulting C^1 surface. Nielson's method is further extended by Pottmann [78] who produced the generalization of MNN to C^r surface. The essential part of the Pottmann's method is the use of a variational principle to define the function values as well as cross-boundary derivatives over the edges of a triangulation of the data points. Based on earlier works by [70] and [78], Kolb and Seidel [53] generated

a triangular network of curves that interpolates the data points at the vertices of the network. A C^2 surface is constructed over the network where the shape can be controlled parametrically and the resulting surface has a uniform appearance i.e. the use of triangular patches with no negative effects on the curvature distribution of the surface as a whole.

Saraga [86] presented a method for constructing a G^1 smooth surface composing of independently parametrized triangular polynomial Bézier patches where all the patches are treated uniformly as having degree 8, to fit scattered data points triangulated in $\mathbf{R}^3$ with arbitrary topology. In order to optimize the shape of a surface, a minimum value of an integral expression or functional of a known function is obtained that depends (not necessarily explicitly) on an unknown function and some of its derivatives subject to the special conditions along the boundary of the global domain.

In this thesis, we propose another simple global interpolating method to fill the triangular patches based on fairness measure of principal curvature norm, which lead us to surfaces which we called *surfaces with minimized principal curvature norm*. We will find an extremum of the integral function in terms of the quadratic form of functionals with respect to the C^1 or G^1 continuity conditions along shared edges and vertices of a triangle. A single quartic Bézier triangular patch is used for this construction.

1.2 Interpolation to Positive Scattered Data

The interpolating methods that we have discussed usually ignore the shape property such as monotonicity ([18], [33], [48], [87], [88], [89]), positivity ([7], [8], [12], [49], [68], [74], [75], [90]) or convexity ([10], [11], [13], [14], [60]) of data

points. Thus, we need to add this characteristic to one of its main conditions and strengthen the chance of preserving the shape of the function. This method is known as shape preserving interpolation where the constructed interpolants obey the shape of the given monotonic, positive and/or convex data. This is a step further regarding the interpolation method as it can fit the shape much better and closer to the given data function than the classical method. Many researchs on shape preserving interpolation methods have been pursued, for example, those on quadratic spline methods ([92], [66], [55]), cubic splines method ([33]) and rational quadratic splines method ([18]). Some of these methods have also been extended to surface fitting.

The main focus on shape preserving interpolation in this thesis is on the preservation of the positivity of data points. The problem of positivity preserving interpolation or the interpolation to positive data by a positive function, is often of interest. This problem could arise if one has data points on one side of a plane, and wishes to have an interpolating surface which is also on the same side of this plane. The significance of positivity lies in the fact that sometimes it does not make sense to talk of some quantity to be negative. For example, in the area of scientific visualization and interpolation of measurements such as rainfall, percentage of mass concentration in a chemical reaction, volume and mass of something which would be meaningless when it is negative. Various methods concerning visualization of positive data of curves and surfaces can be found in the literature (see for example [90], [34], [73], [7], [8], [9], [74], [12], [54], [75]).

Amongst these works, visualisation of positive data using bivariate functions defined on rectangular or triangular meshes can be found for example in Brodlie *et al.* [8], Ong and Wong [74], Chan and Ong [12], and Piah *et al*. [75]. Brodlie *et al*. [8] derived sufficient conditions to ensure a positive piecewise bicubic interpolant is

obtained for positive data. The approach is based on the results of Schmidt and Hess [90] for the univariate case. Specifically, it looks at the problem of constructing a piecewise bicubic function from data on a rectangular mesh, such that this function is non-negative (positive). Sufficient conditions for positivity are derived in terms of the first partial derivatives and mixed partial derivatives at the grid points. These conditions form the basis of a positive interpolation algorithm. Ong and Wong [74] described a local C^1 positivity preserving scheme on triangular mesh using side vertex method for interpolation. The rational cubics are used for univariate interpolation along the line segments joining a vertex to opposite edge of a triangle. The weights of the rational cubics are chosen by using the corresponding univariate results on non-negativity in Goodman *et al*. [34]. The interpolating surface is a convex combination of three triangular patches. Chan and Ong [12] also described a local C^1 non-negative preserving scheme for scattered data defined as piecewise convex combination of cubic triangular Bézier patches. Sufficient conditions for non-negativity of a cubic Bézier triangle are derived and these conditions prescribe lower bounds to the Bezier ordinates. This is done by imposing the same lower bound value for the edge (other than the vertices) and inner Bézier ordinates. Non-negativity is achieved by modifying if necessary the first order partial derivatives at the data sites. Piah *et al*. [75] followed similar approach as in Chan and Ong [12] but offers more relaxed sufficient conditions which are easier to compute on the ordinates of the Bézier control points.

Constraining surfaces to be positive everywhere that interpolates ungridded data has received less attention compared with preserving positivity of curves and surfaces that interpolate gridded data. Thus, motivated by earlier works of Chan and Ong [12], and Piah *et al*. [75], we shall focus on positivity preserving of surface data

defined on ungridded data using triangular patch in this thesis. We will derive sufficient positivity-preserving conditions on Bézier triangular patches and construct bivariate positivity preserving C^2 quintic interpolants to scattered data using convex combination method. However, the disadvantage of this scheme and previous two schemes ([12], [75]) is that the inner and edge Bézier ordinates are assigned the same lower bound. Thus, we are also proposing a new scheme for a C^1 positivity-preserving scheme using cubic triangular Bézier patch by deriving sufficient conditions for the lower bound of the edge ordinates to be adjusted independently and the inner Bézier ordinate depends on the edge ordinates while maintaining the positivity of the triangular patches.

The construction of C^1 cubic and C^2 quintic interpolating surfaces which are only constrained to lie above the *xy*-plane might not be enough if we often have some additional information that we wish to build into the reconstruction which must lie within a specific range although we already know the data points are positive. Various methods concerning visualization of constrained interpolants using bivariate functions can be found. Mulansky and Schmidt [68] constructed a constrained C^1 interpolant using quadratic splines on a Powell–Sabin refinement of the original triangulation. Brodlie *et al.* [8], Ong and Wong [74], Chan and Ong [12] also generalised their results to that of an interpolant subjects to any linear constraint, that is, above or below any plane besides the *xy*-plane. Indeed the surface can be constrained in-between two given planes. Recently Brodlie *et al*. [9] discussed the problem of visualizing data where the underlying constraints must be preserved. They have shown how the modified quadratic Shepard method, which interpolates scattered data of any dimension, can be constrained to preserve positivity. This is done by forcing the quadratic basis functions to be positive. The method can be

extended to handle other types of constraints, including lower bound of 0 and upper bound of 1 as occurs with fractional data. A further extension allows general range restrictions, creating an interpolant that lies between any two specified functions as the lower and upper bounds. Most of these methods have been done on C^1 smooth surfaces but little effort has been spared for C^2 smooth surfaces which have very significant applications in CAGD. Hence, we will extend our proposed C^2 quintic positivity scheme to include a larger set of constraint surfaces besides the plane $z = 0$.

1.3 Thesis Outline

The main work in this thesis focuses on parametric continuous interpolants to functional scattered data by a new global method and the construction of new positivity preserving interpolation schemes including constrained interpolation which are defined on triangular patches. However, we also discuss the geometric continuous interpolants for scattered data as a global approach to fill a triangular patch.

In Chapter 2, we review some of the materials that will be used in later chapters. Some of the materials reviewed are triangulation of data points, methods of gradient estimation, triangular Bézier patch representation and smoothness conditions.

In Chapter 3, we review the works by Goodman and Said [35], Foley and Optiz [27] and Chang and Said [15] for local convex combination method to fill a triangular patch.

In Chapter 4, we will describe our proposed global parametric and geometric continuous interpolants using fairness surface criteria based on principal curvature

norm. The construction of positivity-preserving interpolation will be discussed in Chapter 5 including the implementations of the generalised positivity-preserving scheme using C^2 quintic Bézier triangular patches and a new improved positivity-preserving scheme using C^1 cubic Bézier triangular patches. The implementation of these proposed methods using actual meteorological and geoscience data will be given.

The construction of a new C^2 quintic constrained interpolation is discussed in Chapter 6. Finally, Chapter 7 presents the conclusion and possible research to be pursued beyond the scope of this thesis.

CHAPTER 2
BACKGROUND

2.1 Introduction

This chapter will provide the background knowledge required for the rest of this thesis. We begin by describing a triangulation of data points using Delaunay triangulation in Section 2.2. The gradient estimation methods at vertices of triangles are discussed in Section 2.3. Section 2.4 gives representation of a Bezier triangular patch. Finally, the parametric and geometric continuity between adjacent triangular patches are discussed in Section 2.5.

2.2 Triangulation of Data Points

Triangulation is a fundamental problem in computational geometry, because the first step in working with complicated geometrical objects is to break them into simple geometrical objects. The simplest geometrical objects are triangles in two dimensions, and tetrahedra in three dimensions. Classical applications of triangulation include finite element analysis and computer graphics. A triangulation of a set of points $V = \{v_i = (x_i, y_i)\}_{i=1}^{n}$ consists of vertices, edges (connecting two vertices) and faces (connecting three vertices). The triangulation must satisfy the following properties.

1. The union of all faces including the boundary is the convex hull of all vertices.
2. The intersection of two triangles is either empty, or a common vertex, or a common edge.
3. If *v* is a boundary vertex, then exactly two boundary edges meet at *v*.

One of the popular method for triangulation of data points is the Delaunay triangulation. This triangulation is a dual of a Voronoi diagram. The Voronoi diagram of a point set $V = \{v_1, v_2, \ldots, v_n\}$ is a subdivision of the plane with the property that each Voronoi cell of vertex v_i, $V(v_i)$ contains all locations that are closer to v_i than to every other vertex of V. The vertices V are also called Voronoi generators. Each edge of a Voronoi cell is the bisector of the connection of v_i to the corresponding neighbouring cell. Each intersection of Voronoi edges belongs to at least three Voronoi cells and is the centre of the circle through the generators of these three cells. Delaunay triangulation can be achieved from a Voronoi diagram by connecting vertices, whose regions in the Voronoi diagram intersect (see [6] for further details). Figures 2.1(a) - 2.1(c) show an example of a Voronoi diagram with 32 vertices of interest and its corresponding Delaunay triangulation. The result of using the Delaunay scheme is the triangulation that maximized the minimum angles of all triangles. In other words, in a Delaunay triangulation, the circle that circumscribes three vertices of any triangle contains no other vertices as shown in Figure 2.1(d). It can be seen that the circle C_1 does not include vertex v_4, while the circle C_2 does not contain vertex v_1.

There exist several different techniques for constructing a Delaunay triangulation of a given scattered points such as flipping algorithm ([94]), randomized incremental insertion algorithm ([39]), incremental construction algorithm ([21], [22]), divide-and-conquer algorithm ([17]) and plane sweep algorithm ([26]). In this thesis, we shall use a built-in function (delaunay(x,y)) in MATLAB software which is based on Fortune's plane sweep algorithm ([26]) for Voronoi diagram to triangulate a given 2D data points.

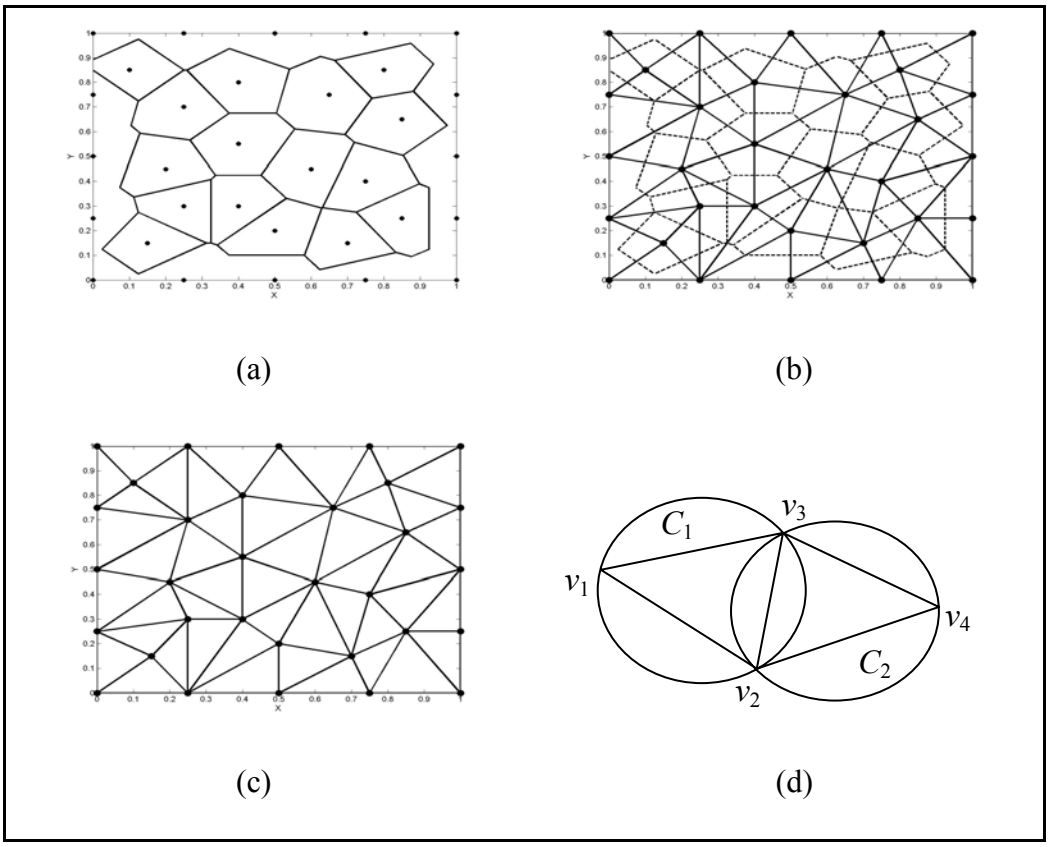

Figure 2.1. (a) Voronoi diagram (b) Delaunay triangulation with its Voronoi diagram (c) Delaunay triangulation (d) Concept of Delaunay triangulation.

2.3 Gradient Estimation Methods

There are several methods in the literature which can be used to estimate the gradients at data points in the plane. Most of the methods known in the literature for numerical evaluation of the partial derivatives of a function are the least-squares minimization methods ([81], [58]), weighted average of the slopes of planes through some of the prescribed function values ([1], [52]) and convex combination of derivatives on all triangular planes of which the point is a vertex ([36]). In this section we will discuss the method of convex combination ([36]) to estimate first order derivatives at vertices of triangle which is used in this thesis due to its simplicity to handle, stability, requires less computation times and has comparable accuracy to the other mentioned methods of gradient estimation. However the

drawback of this method is that it is only applicable for first order derivatives estimation but not for second and higher order derivatives estimate. Thus, for the second order partial derivatives estimation, we shall use method based on least squares minimization with best fitting quadric surface. These two methods are described as follows.

2.3.1 Convex Combination Method ([36])

First assume that a node V is in the interior of the triangulation domain and let $T_i,\ i = 1, \ldots, k$ where k is the number of triangles in the triangulation mesh which have V as a vertex (see Figure 2.2, for $k = 5$).

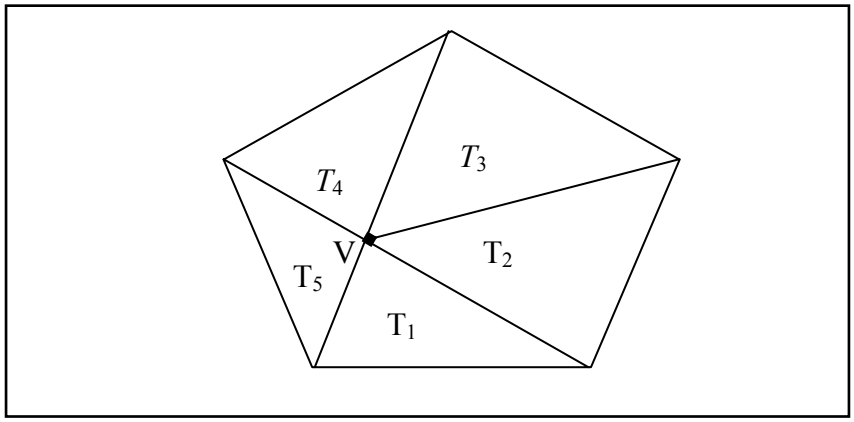

Figure 2.2. Triangles in a triangulation ($k = 5$)

For $i = 1, \ldots, k$, we denote g_i as the gradient of the linear interpolant to the data at vertices of T_i. The gradient of function F at V, $\nabla F = \left(\frac{\partial F}{\partial x}, \frac{\partial F}{\partial y} \right)$ is a convex combination of g_i can be written as

$$\nabla F = \frac{\sum_{i=1}^{k} \frac{1}{A_i} g_i}{\sum_{i=1}^{k} \frac{1}{A_i}} \tag{2.1}$$

where $A_i,\ i = 1, \ldots, k$ denotes the area of the triangle T_i.

Suppose that a triangle T_i has vertices $(x_j^{\,i}, y_j^{\,i})$ with corresponding data values z_j, $j = 1, 2, 3$. Then the linear interpolant to these points is a plane $a_i x + b_i y + c_i z + d_i = 0, i = 1, \ldots, k$ where a_i, b_i and c_i are components of the plane's normal vector (Figure 2.3).

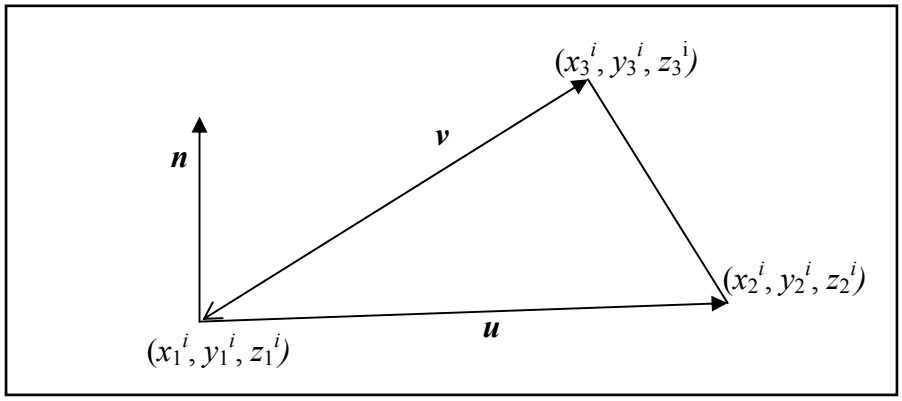

Figure 2.3. Vector plane of linear interpolant to the data at vertices of T_i

The normal vector of the plane is $\mathbf{n} = \mathbf{u} \times \mathbf{v} = a_i \mathbf{i} + b_i \mathbf{j} + c_i \mathbf{k}$ where

$a_i = (y_2^{\,i} - y_1^{\,i})(z_3^{\,i} - z_1^{\,i}) - (y_3^{\,i} - y_1^{\,i})(z_2^{\,i} - z_1^{\,i})$, $b_i = (x_3^{\,i} - x_1^{\,i})(z_2^{\,i} - z_1^{\,i}) - (x_2^{\,i} - x_1^{\,i})(z_3 - z_1^{\,i})$,

$c_i = (x_2^{\,i} - x_1^{\,i})(y_3^{\,i} - y_1^{\,i}) - (x_3^{\,i} - x_1^{\,i})(y_2^{\,i} - y_1^{\,i})$ and $\mathbf{i}$, $\mathbf{j}$, $\mathbf{k}$ are the unit vectors.

Thus, the gradient of the plane is $g_i = (\frac{\partial z}{\partial x}, \frac{\partial z}{\partial y}) = (-\frac{a_i}{c_i}, -\frac{b_i}{c_i})$ and the area of triangle T_i is $A_i = \frac{1}{2}|c_i|$. From (2.1), the gradient at an interior node of triangulation is

$$\left(\frac{\partial z}{\partial x}, \frac{\partial z}{\partial y}\right) = \frac{\sum_{i=1}^{k} \frac{1}{|c_i|}\left(-\frac{a_i}{c_i}, -\frac{b_i}{c_i}\right)}{\sum_{i=1}^{k} \frac{1}{|c_i|}}. \qquad (2.2)$$

When V is a node on the boundary of the domain (Figure 2.4), the estimated gradient is

$$\nabla F = \frac{\sum_{i=1}^{k} \frac{1}{A_i} \{ \frac{(2A_i + A_i')g_i - A_i g_i'}{A_i + A_i'} \}}{\sum_{i=1}^{k} \frac{1}{A_i}} \tag{2.3}$$

where $i = 1, \ldots, k$, A_i' is the area of T_i' and g_i' is the gradient of the linear interpolant over T_i' with T_i' is the triangle not containing V but shares the edge of T_i. (2.3) also can be expressed as

$$\left(\frac{\partial z}{\partial x}, \frac{\partial z}{\partial y} \right) = \frac{\sum_{i=1}^{k} \left(\frac{(2|c_i| + |c_i'|)\left(-\frac{a_i}{c_i}, -\frac{b_i}{c_i} \right) - |c_i| \left(-\frac{a_i'}{c_i'}, -\frac{b_i'}{c_i'} \right)}{|c_i|(|c_i| + |c_i'|)} \right)}{\sum_{i=1}^{k} \frac{1}{|c_i|}} \tag{2.4}$$

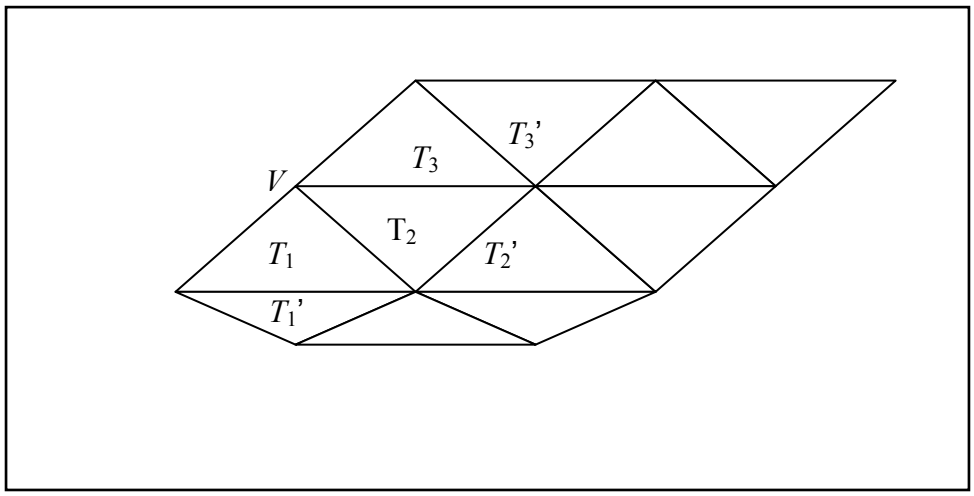

Figure 2.4. Node V on the boundary of the domain

2.3.2 Method Based on Least Square Minimization ([81])

We can interpolate the current data point and approximate its nearest neighbours with a simple known surface such as a sphere, an ellipsoid, or a quadric surface. This surface can be found by well-known least squares minimization technique. The partial derivative at current data point is then defined to be the partial derivatives of this approximation surface at that point. In this thesis, we will use best-fitting quadratic surfaces defined as

$$f(x,y) = ax^2 + bxy + cy^2 + dx + ey + f \tag{2.5}$$

where a, b, c, d, e and f are the coefficients to be determined.

Let the vertex P_0 of the triangular mesh surrounded by vertices $P_1(x_1, y_1)$, $P_2(x_2, y_2)$, . . . , $P_k(x_k, y_k)$ and the height of the vertices $\{P_0, P_1, \ldots, P_k\}$ are represented by $\{z_0, z_1, \ldots, z_k\}$ as shown in Figure 2.5. We turn our attention to the vertex which corresponds to $P_0(x_0, y_0)$. Other vertices can be dealt with in a similar way. We can derive the first and second order partial derivative at P_0 as $F_x(P_0) = 2ax_0 + by_0 + d$, $F_y(P_0) = bx_0 + 2cy_0 + e$, $f_{xx} = 2a$, $f_{yy} = 2c$ and $f_{xy} = b$.

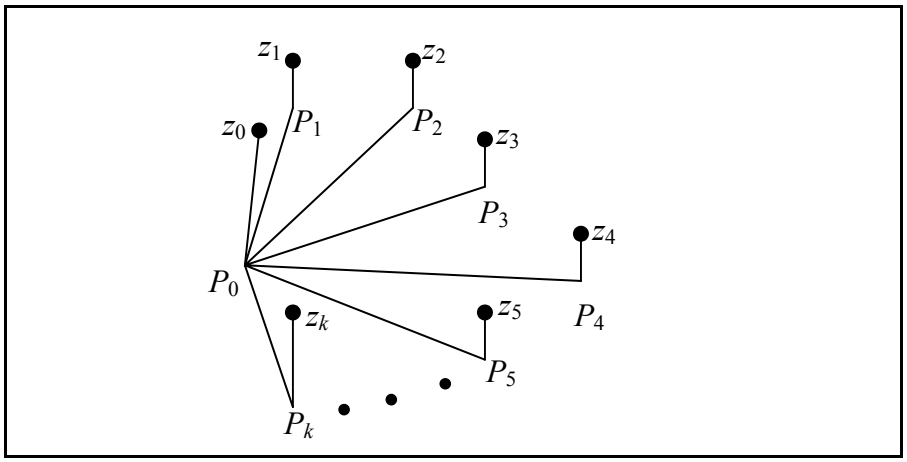

Figure 2.5. k vertices surrounding vertex P_0

Substitute $P_0, P_1, \ldots, P_k$ and $z_0, z_1, \ldots, z_k$ in (2.5), we obtain a linear system

$$U\mathbf{c} = \mathbf{z} \tag{2.6}$$

where

$$U = \begin{bmatrix} x_0^2 & x_0y_0 & y_0^2 & x_0 & y_0 & 1 \\ x_1^2 & x_1y_1 & y_1^2 & x_1 & y_1 & 1 \\ . & . & . & . & . & 1 \\ . & . & . & . & . & 1 \\ . & . & . & . & . & 1 \\ x_k^2 & x_ky_k & y_k^2 & x_k & y_k & 1 \end{bmatrix}, \quad \mathbf{c} = \begin{bmatrix} a \\ b \\ c \\ d \\ e \\ f \end{bmatrix} \quad \text{and} \quad \mathbf{z} = \begin{bmatrix} z_0 \\ z_1 \\ . \\ . \\ . \\ z_k \end{bmatrix}.$$

Theorem 2.1.

Consider the (m x n) system $A\mathbf{x} = \mathbf{b}$

(a) The associated system $A^TA\mathbf{x} = A^T\mathbf{b}$ is always consistent

(b) The least-squares solutions of $A\mathbf{x} = \mathbf{b}$ are precisely the solutions of $A^TA\mathbf{x} = A^T\mathbf{b}$

(c) The least square solution is unique if and only if rank $A = n$.

Proof of the Theorem 2.1 can be found in Johnson *et al*. ([50]). Applying the above theorem on (2.6), the values of a, b, c, d, e and f can be obtained, that is,

$$\mathbf{c} = (U^T U)^{-1} U^T \mathbf{z} \tag{2.7}$$

and the values of F_x, F_y, F_{xx}, F_{yy}, F_{xy} at vertex P_0 can then be calculated.

Note that, if matrix U in (2.6) is in the form of rank deficient matrix (that is rank of U is less than number of unknowns) or the number of points surrounding P_0 is less than five, we can approximate the solution (2.7) by using the pseudo-inverse of U in the least square method (see [50] for further details).

2.4 Representation with Bézier Triangular Patches

A review of the basic mathematics of Bézier triangular patch as described in Farin [24] will be given in this section.

2.4.1 Barycentric Coordinates

Since we are working with triangles, we will utilise barycentric coordinates rather than Cartesian coordinates. Let T be a triangle with vertices $V_i = (x_i, y_i)$, $i = 1, 2, 3$ (Figure 2.6). Any point $V = (x, y) \in R^2$ can be expressed as

$$V = rV_1 + sV_2 + tV_3 \tag{2.8}$$

where $r + s + t = 1$ that is equivalent to a linear system

$$A\mathbf{x} = \mathbf{b} \tag{2.9}$$

with $A = \begin{bmatrix} 1 & 1 & 1 \\ x_1 & x_2 & x_3 \\ y_1 & y_2 & y_3 \end{bmatrix}$ is a non-singular Vandermonde matrix, $\mathbf{x} = \begin{bmatrix} r \\ s \\ t \end{bmatrix}$ and $\mathbf{b} = \begin{bmatrix} 1 \\ x \\ y \end{bmatrix}$.

The point V is said to have barycentric coordinates (r, s, t) with respect to triangle T.

Solving (2.9) using Cramer's rule, we obtain

$$r = \frac{(x_2y_3 - y_2x_3) - x(y_3 - y_2) + y(x_3 - x_2)}{\Delta} \tag{2.10}$$

$$s = \frac{(x_1y_3 - y_1x_3) - x(y_3 - y_1) + y(x_3 - x_1)}{\Delta} \tag{2.11}$$

$$t = \frac{(x_1y_2 - y_1x_2) - x(y_2 - y_1) + y(x_2 - x_1)}{\Delta}. \tag{2.12}$$

where Δ is a determinant of A. From (2.10)-(2.12), it is apparent that each of the barycentric coordinates is a linear polynomial in x and y. Note that, the interior of the triangle is characterised by the additional restriction, $r, s, t > 0$.

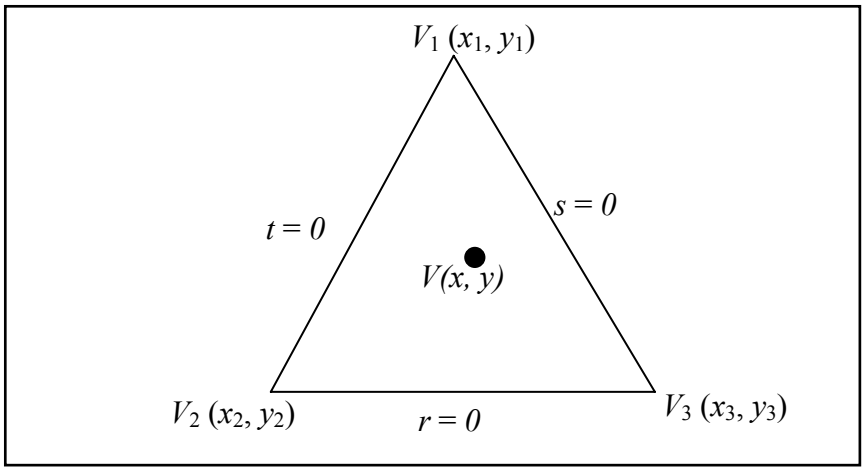

Figure 2.6. Barycentric coordinates

2.4.2 Bézier Triangular Patches

Bézier Triangular patches or Bézier triangles are the true generalisation of Bézier curves to a surface form. In practice, the tensor product Bézier patch have received more attention due to their prevalent use in industry. However, triangular patches have much to offer. One important offering is the ability to model objects with arbitrary topology especially for the problem of fitting smooth surfaces to scattered data. A degree-n Bézier triangular patch P on T is defined as

$$P_n(r, s, t) = \sum_{\substack{i+j+k=n \\ i\geq 0,\, j\geq 0, k\geq 0}} b_{ijk} B_{ijk}^n(r, s, t) \tag{2.13}$$

where b_{ijk} are the Bézier ordinates or control points of P and

$$B_{ijk}^n(r, s, t) = \frac{n!}{i!\, j!k!} r^i s^j t^k \quad , i + j + k = n,\ i,\ j,\ k \geq 0. \tag{2.14}$$

are bivariate Bernstein basis polynomials of degree-n relative to triangle T. Equation (2.14) is indeed bivariate because one variable is dependent on the other two, $t = 1 - r - s$.

2.4.3 Derivatives of Bézier Triangular Patches

We also need a formula for the derivative of $P(r, s, t)$. For a given direction represented by the vector $d=(d_1, d_2, d_3)$, $d_1+d_2+d_3=0$, the directional derivative

$$D_d P(r, s, t) = d_1 \frac{\partial P}{\partial r} + d_2 \frac{\partial P}{\partial s} + d_3 \frac{\partial P}{\partial t}.$$

In general l-th order derivative of $P(r, s, t)$ is, ([59])

$$D_{d^l} P(r, s, t) = \frac{n!}{(n-l)!} \sum_{i+j+k=n-l} C^l_{i,j,k}(d) B^{n-l}_{i,j,k}(r, s, t) \tag{2.15}$$

where $B^{n-l}_{i,j,k}(r, s, t)$ is (2.14) and

$$C^m_{i,j,k}(d) = d_1 C^{m-1}_{i+1,j,k}(d) + d_2 C^{m-1}_{i,j+1,k}(d) + d_3 C^{m-1}_{i,j,k+1}(d) \tag{2.16}$$

with $C^0_{i,j,k}(d) = b_{i,j,k}$, $i+j+k=n$.

Also its lth mixed directional derivative with respect to directions $d = (d_1, d_2, d_3)$ and $e = (e_1, e_2, e_3)$, $e_1 + e_2 + e_3 = 0$ is, ([15])

$$D^l_{d^{l_1} e^{l_2}} P(r,s,t) = \frac{n!}{(n-l_1-l_2)!} \sum_{i+j+k=n-l} \sum_{\substack{\lambda_1+\lambda_2+\lambda_3=l_1 \\ \lambda_4+\lambda_5+\lambda_6=l_2 \\ l_1+l_2=l}} b_{i+\lambda_1+\lambda_4, j+\lambda_2+\lambda_5, k+\lambda_3+\lambda_6} B^{l_1}_{\lambda_1,\lambda_2,\lambda_3}(d) B^{l_2}_{\lambda_4,\lambda_5,\lambda_6}(e) B^{n-l}_{i,j,k}(r, s, t) \tag{2.17}$$

where $B^{l_1}_{\lambda_1,\lambda_2,\lambda_3}(d)$, $B^{l_2}_{\lambda_4,\lambda_5,\lambda_6}(e)$ and $B^{n-l}_{i,j,k}(r, s, t)$ are given by (2.14).

2.5 Smoothness Conditions

In order to create a smooth surface through the data points there must be a smooth transition from one patch to another across all shared edges and thus the certain smoothness conditions need to be satisfied. The derivation and further details of smoothness criteria given in this section can be found in Farin ([24], [25]) and Lai [56].